



OPEN Lateral frontopolar theta-band activity supports flexible switching between emotion regulation strategies

Agnieszka K. Adamczyk^{1,2}✉, Bob Bramson^{2,3}, Saskia B. J. Koch³, Mirosław Wyczesany¹, Jacobien M. van Peer² & Karin Roelofs^{2,3}

Flexible emotion regulation is essential for mental health and well-being. However, neurocognitive mechanisms supporting emotion regulation flexibility remain unclear. Lateral frontal pole (FPI) contributes to flexible behavior by monitoring the efficacy of alternative strategies. This preregistered study examines if FPI also supports flexible use of emotion regulation strategies. It focuses on pre-decision theta-band activity as a potential indicator of this adaptive process. Sixty-three participants performed an emotion regulation strategy-switching task, involving three phases: (1) implementing an instructed (reappraisal or distraction) strategy, (2) deciding whether to 'maintain' the current or 'switch' to the alternative strategy, and (3) implementing the chosen strategy. Results showed that switching is predicted by the reduced efficacy of an initial emotion regulation strategy (indexed with EMG corrugator activity) and is made in accordance with situational demands (stimulus reappraisal affordances). Critically, switching to an alternative emotion regulation strategy is associated with increased theta-band power in FPI around the time of the decision. These findings support the previously established role of FPI theta-band activity in monitoring counterfactual efficacy of alternative strategies. Crucially, they extend this notion to cognitive emotion regulation, thereby offering promising neural targets for stimulation-based therapies aimed at enhancing emotion regulation flexibility in affective psychopathologies.

Keywords Emotion regulation flexibility, Cognitive reappraisal, Attentional distraction, Lateral frontal pole, Anterior prefrontal cortex

Emotion regulation flexibility, the ability to shift regulatory strategies when the current implementation falls short, is central to well-being^{1,2}. Choosing between emotion regulation strategies requires comparing the efficacy of the current strategy with that of alternative strategies. Converging evidence suggests that the frontopolar cortex is implicated in monitoring and evaluating the validity of current (medial part) and alternative tasks (lateral part), enabling flexible switching between them³. Indeed, functional magnetic resonance imaging (fMRI) studies show that lateral frontal pole (FPI) is consistently active when individuals: perform emotion regulation tasks that allow the use of multiple versus single emotion regulation strategies⁴; implement controlled vs. automatic emotional actions in emotional approach-avoidance tasks^{5,6}; and arbitrate between alternative decisions to maximize rewards in reinforcement learning tasks^{7,8}. Based on these insights, recent emotion regulation theories, such as flexible emotional control theory (FECT)^{4,9}, have proposed that FPI monitors the counterfactual efficacy of concurrently available emotion regulation strategies (i.e., the efficacy of the strategies that could have been implemented instead), driving the decision to switch to an alternative strategy when the current strategy is ineffective or suboptimal for the given situational demands. However, no prior studies have investigated whether FPI is indeed involved in switching between emotion regulation strategies. Here, we aim to investigate whether FPI activity, previously associated with behavioral strategy-switching¹⁰⁻¹², is also implicated in emotion regulation strategy-switching. Such evidence would provide direct support for the role of counterfactual monitoring processes in flexible emotion regulation, as proposed by FECT^{4,9}. Moreover, it could

¹Psychophysiology Laboratory, Institute of Psychology, Jagiellonian University, Krakow, Poland. ²Experimental Psychopathology and Treatment, Behavioural Science Institute, Radboud University, Nijmegen, The Netherlands. ³Affective Neuroscience, Donders Centre for Cognitive Neuroimaging, Radboud University, Nijmegen, The Netherlands. ✉email: agnieszka.adamczyk@ru.nl

suggest a potential neural target for brain stimulation protocols for conditions in which emotion regulation falls short.

In this preregistered study, we focused on theta-band activity in FPL, given the well-established role of frontopolar theta oscillations in higher-order (meta-)cognitive processes^{11,13–16}, including various forms of top-down control, such as emotional action control^{5,10}. Frontopolar theta-band oscillations are thought to organize local and long-range neural activity by temporally releasing neurons from inhibition, creating overlapping periods of excitability across the neuronal network involved in the execution of a particular task^{12,17}. Theta-band activity in FPL has been associated with control over social-emotional behavior, particularly when a prepotent emotional response has to be overridden in favor of an alternative action^{5,10}. Furthermore, during reward-based reinforcement learning, FPL theta-band power increases before a switch to an alternative, explorative action¹¹. These observations fit with the hypothesized role of FPL in monitoring the potential benefit of counterfactual strategies^{4,7}. This function might be especially relevant for emotion regulation, where the congruency between the current emotional state and the emotion regulation goal has to be evaluated and integrated into regulatory decisions, a role for which FPL is well-suited¹⁸. Such integration of goal representations with emotional information is essential for flexible and context-sensitive behavior¹⁹. However, this hypothesized role of FPL theta in emotion regulation strategy monitoring and switching remains to be empirically determined. The primary goal of this study was to therefore test whether increased theta-band power over FPL is associated with flexible decisions to switch to an alternative emotion regulation strategy, extending the established role of FPL in counterfactual decision-making to cognitive emotion regulation.

When evidence in favor of the alternative strategy increases during decision making, FPL may influence downstream activity in posterior parietal cortex (PPC), a region hypothesized to implement switching⁷. Specifically, FPL increases functional connectivity with PPC before the implementation of switching in value-based reinforcement-learning paradigms. Moreover, when selecting alternative emotional actions, FPL increases interregional communication with downstream parieto-frontal areas that are implicated in action execution¹⁰. This is reflected in modulations of gamma-band activity in sensorimotor cortex, by the phase of theta-band oscillations in FPL. We thus additionally tested coupling between the theta-phase in FPL and gamma-power in PPC during decisions to switch to the alternative vs. maintaining the current emotion regulation strategy.

To test the predicted role of FPL in flexible emotion regulation, we re-analyzed data from a previous preregistered EEG/EMG study²⁰, now with a specific focus on neural oscillatory activity during the decision to switch emotion regulation strategies. Sixty-three participants were taught two emotion regulation strategies: Distraction and reappraisal^{21–23}. Reappraisal involved changing the meaning of the depicted negative situation (reinterpretation type of reappraisal), whereas distraction involved thinking of something neutral and unrelated to this situation^{22,24,25}. We chose these two cognitive strategies as they constitute the most commonly investigated forms of emotion regulation, and they have been used in prior work on strategy monitoring and switching^{26,27}. Moreover, both these strategies are frequently used in everyday life as well as clinical practice^{28,29}, yet their efficacy seems to be differently moderated by various cognitive (e.g., working memory load)³⁰ and situational factors (e.g., stimulus intensity)^{25,31,32}. This complementary, context-dependent efficacy makes them useful to study flexible strategy-switching decisions.

On each trial (Fig. 1D), participants first implemented an initial (instructed) emotion regulation strategy while seeing a highly arousing negative picture and then decided whether they wanted to maintain this current strategy or switch to the alternative strategy. Subsequently, the picture was presented again and participants were asked to implement the chosen (reappraisal or distraction) strategy (cf.²⁷). To induce switching between these strategies, we presented pictures that were either easy or difficult to reinterpret (high or low *reappraisal affordance* level, respectively; cf.³³). Reappraisal affordance is defined as the opportunities for semantic reinterpretation that are inherent in a stimulus^{33,34}. For instance, an image of a crying child sitting at the table offers more opportunities for reappraisal (e.g., a child did not want to stop playing with a friend to eat dinner) and is thus easier to reappraise than an image of a homeless person facing the ground (as the aversive meaning is unequivocal). Thus, the former image has higher reappraisal affordances than the latter (see examples from Fig. 1A). Here, reappraisal affordances were manipulated by selecting pictures based on how subjectively easy and effective it was to reappraise them, which was determined in a separate pilot study (see our preregistration and the Method section for details).

First, we verified whether switching was made in accordance with reappraisal affordance and whether it was predicted by the reduced efficacy of the initial emotion regulation strategy, based on facial electromyography (EMG) corrugator supercilii activity. EMG corrugator activity is a well-established marker of negative affect³⁵ that is a robust measure of emotion regulation efficacy^{36–38} and that has recently been shown to predict switching between reappraisal and distraction strategies^{20,26}. Then, we applied time–frequency and source reconstruction analyses, to assess increases in FPL theta-power, as well as connectivity analyses, to test the increased FPL theta-PPC gamma coupling, for trials where individuals decided to switch vs. maintain the emotion regulation strategy.

Results

Participants switch more when current emotion regulation strategy is less effective

Participants switched on 32.1% ($SD=12.9\%$) of the trials, and significantly more often when the instructed strategy was suboptimal for the stimulus category (reappraisal affordance), i.e. from distraction to reappraisal in response to high affordance pictures, and vice versa for low affordance pictures (see Fig. 1B); strategy by affordance interaction, $\chi^2(1)=59.8$, $p<0.0001$, odds ratio=10.9. Moreover, switching (vs. maintaining) the instructed strategy was preceded by increased corrugator activity (i.e., increased negative affect) during the initial strategy implementation phase (see Fig. 1C), $F(1, 54.9)=6.65$, $p=0.013$, $d=0.64$, suggesting reduced efficacy of the initial strategy in downregulating negative affect. There was no general preference for one strategy over the other ($M_{\text{switch-to-reappraisal}}=35.5$, $M_{\text{switch-to-distraction}}=28.8$), main effect of strategy on switching decisions,

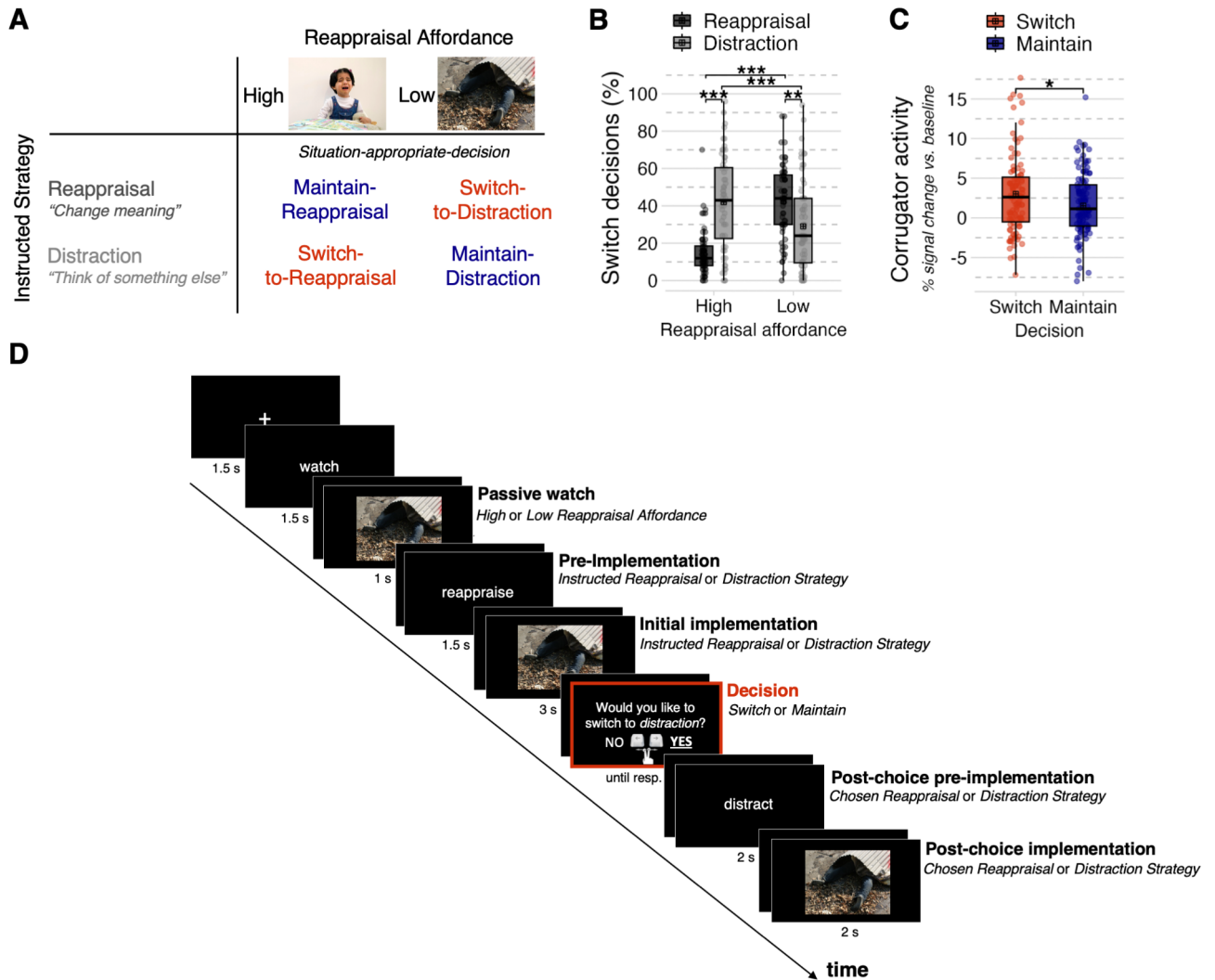


Fig. 1. Emotion regulation strategy switching task, behavioral and peripheral physiological results. **(A)** Manipulation of Reappraisal Affordances: High Affordance pictures were expected to evoke Maintain-Reappraisal and Switch-to-Reappraisal decisions, and Low Affordance pictures Maintain-Distraction and Switch-to-Distraction decisions. **(B)** Reappraisal Affordance induced the expected switching between emotion regulation strategies (see **A**). **(C)** Switching from an instructed strategy was predicted by increased EMG corrugator peripheral physiological activity during initial strategy implementation, suggesting reduced strategy efficacy in downregulating emotional responses. Boxplots show significance of simple effects comprising a significant Instructed Strategy x Reappraisal Affordance interaction (see **B**) and the main effect of Decision on corrugator activity (see **C**). Squares inside the box indicate the group mean, individual participants' results are shown as a scatterplot along the whisker. *** $p < 0.001$, ** $p < 0.003$, * $p < 0.02$. **(D)** Emotion Regulation Switching Task: Sample trial structure. Presentation duration of the pictures and instruction was fixed. Duration of the fixation cross varied between 1.25 and 1.75 s ($M = 1.5$ s). Inter-stimulus intervals (blank screen) varied between 0.3 and 0.7 s ($M = 0.5$ s). The red box outline marks the decision trial phase for which the EEG results are reported (see Fig. 2).

$p = 0.12$. Together, these results confirm that switching to the alternative emotion regulation strategy was made in accordance with situational demands (affordances) and was predicted by reduced efficacy of the initial emotion regulation strategy.

Theta-band power increases in lateral frontopolar cortex prior to switch decisions.

As compared to a baseline window (-1.2 s to -1 s relative to response onset), theta-band power increased over all frontal electrodes prior to making a decision to switch or maintain the current strategy; $p < 0.0001$, 26 channels, -0.95 s to 0.20 s relative to response onset, Fig. 2A–C. Notably, this increase was stronger over left lateral frontal channels in trials leading up to a switch as compared to a maintain decision; $p = 0.029$, 9 channels; 2–6 Hz, -0.25 to 0.20 s relative to response onset, Fig. 2D–F. Reconstructing the cortical sources of this difference showed increases in theta-band activity ($4 \text{ Hz} \pm 2 \text{ Hz}$ of smoothing) over the left lateral frontopolar cortex and temporal-

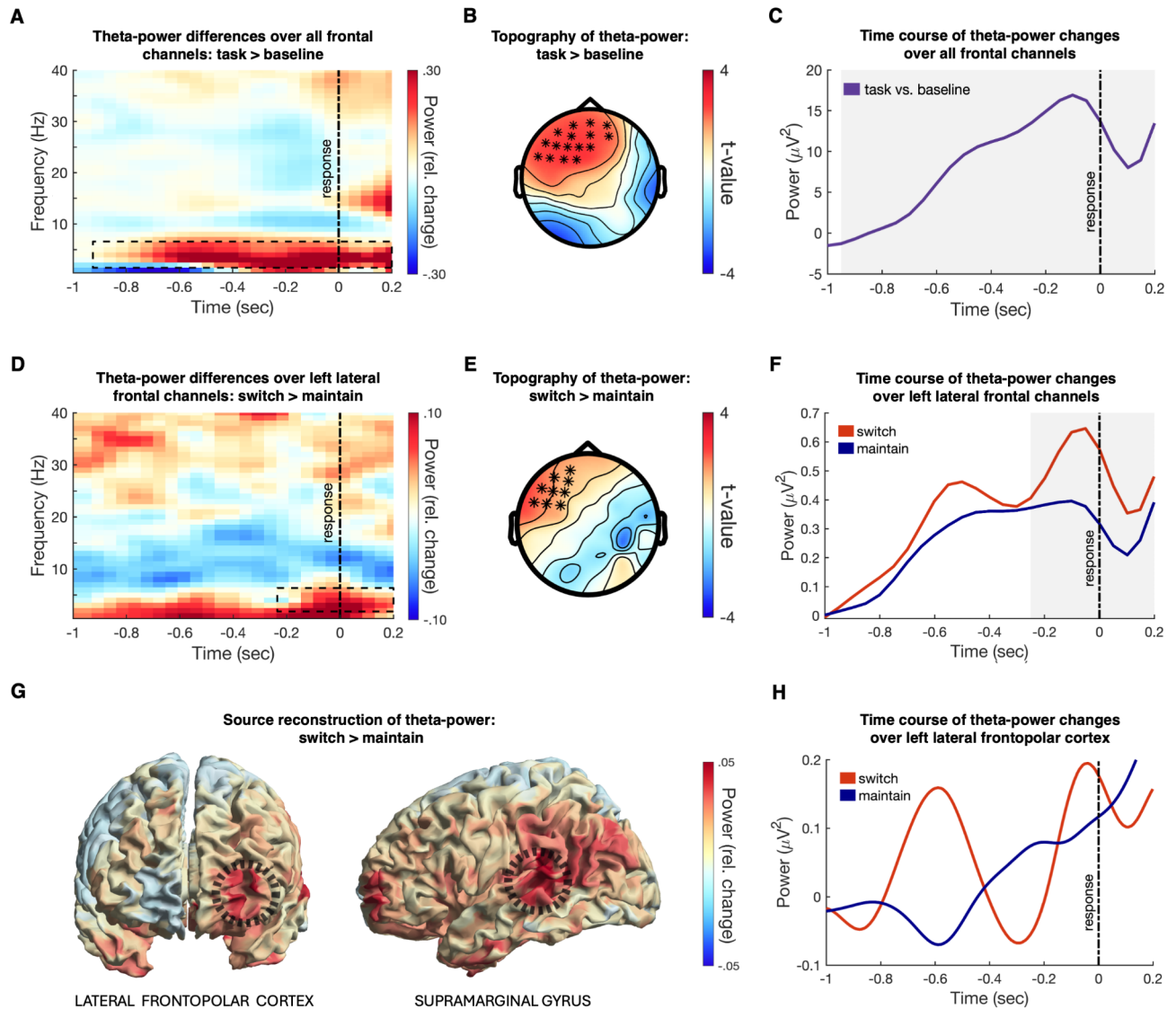


Fig. 2. Decision to switch strategies increases theta-band power in left lateral frontopolar cortex. **(A)** Time–frequency plot of grand average changes in power across all trials (-1 sec before to 0.2 s after response) compared to a baseline period (-1.2 to -1 s before response) averaged over all frontal channels. The dashed box shows the interval with a significant increase in theta-band activity (-0.95 s before to 0.2 s after response; 2–6 Hz). **(B)** Topographic distribution of channels with a significant theta power difference: Task vs. baseline. Please note that this plot shows t-values, and the corresponding channel significance (marked with asterisks), averaged over time-window and frequencies for which the significant theta power increase was observed (see A). Thus, frontal channels with the most consistent theta power differences across time and frequencies are shown as significant (N = 16 out of 26). **(C)** Baseline-corrected changes over time in theta-band power (2–6 Hz) averaged across significant channels and both conditions. The epoch with a significant difference in theta activity as compared to baseline is marked in grey. **(D)** Time–frequency plot of relative power differences between task conditions (switch vs. maintain) averaged over channels with a significant effect (see E). The dashed box shows the interval with a significant switch effect (-0.25 s before to 0.2 s after response; 2–6 Hz). **(E)** Topographic distribution of channels with a significant switch effect (asterisks). **(F)** Changes over time in theta-band power (2–6 Hz) averaged across significant channels (see E). The epoch with a significant difference between the switch vs. maintain condition is marked in grey. **(G)** Cortical distribution of theta-band (4 Hz) switch effects at the source level (frontal and left view). The dashed circles indicate locations from which the theta-band activity was extracted for the connectivity analyses. **(H)** Time series of 2–6 Hz activity extracted from left lateral frontopolar cortex (MNI: -32 66 0; see G).

parietal areas (Fig. 2G). A grid point of the peak frontal increase in theta-band power was identified as the left frontal pole/anterior prefrontal cortex (MNI: -32 66 0; Fig. 2H) and of the peak temporal-parietal increase as left superior temporal gyrus/supramarginal gyrus [SMG; (MNI: -52 -44 16)]. As preregistered, we also verified whether theta-band power increases in medial frontopolar cortex (FPM) when deciding to maintain vs. switch

emotion regulation strategy^{4,9}. There were no clusters indicating an increase in theta-band activity over medial frontopolar cortex (FPM) in the maintain vs. switch condition.

Neural coupling between frontopolar and downstream parietal and temporal cortices.

We next tested the hypothesis that FPI increases neuronal coupling with PPC when participants decide to switch from vs. maintain an instructed strategy. There was no statistically significant task vs. baseline difference in gamma-band power (40–90 Hz) over parietal channels ($N=11$), $p=0.060$. Moreover, the decision to switch vs. maintain a strategy did not increase gamma-band activity in the PPC (source reconstruction defined as average activity of inferior and superior parietal lobules; see Method section for details) in the time-window of increased theta-band activity (–0.95 to 0.2 s relative to response onset). However, given that frontopolar theta might increase timing rather than firing rates of the gamma-band activity³⁹, we calculated phase-amplitude coupling (PAC) between 4 Hz theta oscillations in FPI and reconstructed gamma-band power over PPC for switch and maintain trials and compared PAC between switch and maintain trials using Modulation Index⁴⁰. We also compared potential modulation of PPC excitability in different phases of FPI theta-band signal, as estimated through the slope of the power spectrum for switch versus maintain trials⁴¹. Both methods did not result in statistically significant modulation of PPC activity/excitability by the FPI theta-band phase, $p>0.08$. Finally, we explored phase synchronization between FPI and SMG (which also showed increased theta-band power) with imaginary part of coherency (iCoh)⁴² and phase-slope index (PSI)⁴³. Neither iCoh nor PSI revealed a significantly stronger synchronization in the theta-band (4 Hz) in switch versus maintain trials around the time of the decision, $p>0.49$.

Discussion

This study investigated cortical oscillatory mechanisms supporting flexible switching decisions between alternative emotion regulation strategies. Our principal result is that FPI, a region involved in monitoring and switching between alternative *behavioral* strategies based on their possible advantages over the current strategy, is also involved in switching between *cognitive emotion regulation* strategies. Concretely, just before participants decide to switch to the alternative emotion regulation strategy, theta-band power increases over FPI, compared to when participants maintain the current strategy. This finding provides novel evidence for the involvement of FPI in emotion regulation strategy-switching.

Frontopolar theta-band activity supports exploration of alternative emotion regulation strategies

Our primary finding of increased FPI theta-band power before switch vs. maintain decisions supports the notion that this region is implicated in switching to an alternative emotion regulation strategy^{4,9}. FPI has been involved in monitoring the relative benefit of counterfactual options in cognitive decision-making studies which enables rapid adjustment of behavior when the current strategy becomes unreliable^{3,7,8}. Recent evidence shows that this extends to instances where goal-directed and affective information has to be combined to inform appropriate strategies¹⁸. FPI is especially well-suited for this role, given its access to both lateral and medial circuits⁴⁴, and direct connections from the amygdala complex^{6,45}. Indeed, a meta-analysis of 77 fMRI studies on cognitive emotion regulation showed that FPI is active when participants are allowed to use multiple (vs. single) emotion regulation strategies ($N=42$ studies)⁴. Similarly, FPI is implicated in emotional action control, when participants select alternative (emotion-incongruent) vs. automatic (emotion-congruent) strategies^{5,46}.

Our behavioral and EMG corrugator results show that strategy-switching decisions are not random but are predominantly made in response to stimuli for which the current (instructed) emotion regulation strategy was suboptimal, as shown by the strategy by affordance effect on switching, or ineffective, as shown by increased EMG corrugator amplitudes during initial strategy implementation in switch vs. maintain trials. This increased corrugator activity, a marker of negative affect, might reflect decreased emotion regulation success, after which FPI signals a switch. Putatively, FPI integrates information about the current strategy efficacy (emotional state) with the (regulation) goal state, which serves as counterfactual evidence for switching strategies. That is, increased FPI theta-band power observed immediately before the decision to switch (vs. maintain) an emotion regulation strategy might reflect the process of weighing the evidence for the alternative relative to the current strategy, which directly drives the switching decision^{4,9}. This interpretation is in line with prior studies showing increased frontopolar theta power before switching to an alternative strategy in a reward-based reinforcement learning paradigm¹¹, and before selecting alternative, rule-based actions in an emotional action control paradigm^{5,10}, where emotion–goal integration is critical for flexible goal-directed behavior.

Theoretical accounts suggested that FPI continuously monitors the relative advantage of switching to an alternative strategy^{3,4,9}. We thus expected that FPI would be involved in monitoring the relative advantage of switching to the alternative ER strategy already during initial strategy implementation. We did however not find evidence for increased FPI theta-band activity in the switch vs. maintain condition during this trial phase. It might be that in our study evidence for the strategies was not accumulated/evaluated until after the completion of the strategy implementation. This is in agreement with previous value-based decision-making studies, where FPI activity peaked around the time of the decision (i.e., response) to switch to the alternative strategy^{7,11}.

FPI connectivity with other brain circuits

When an alternative strategy becomes favorable, FPI might relay that information to downstream regions, such as PPC, by creating overlapping periods of excitability through theta-band synchronous activity, implementing the switch^{10,12,47}. In this study, however, we did not observe convincing evidence for the hypothesized FPI theta-PPC gamma coupling. It is important to emphasize that we took several measures to mitigate the possibility that these null results were due to low statistical power. First, we excluded participants that lacked a minimum

preregistered number of trials per condition. Second, we applied orthogonal Slepian sequence tapers for frequencies above 40 Hz, which are designed to increase signal-to-noise ratio (SNR) by reducing the variance of the signal thanks to spectral smoothing. This multi-taper method is especially useful for lower trial counts as well as broadband EEG activity that usually has a higher variability. Finally, as an additional artifact rejection step, we inspected all individual time–frequency plots computed for parietal channels to identify individuals who had strong motor-related artifacts in the gamma range around the time of response. Given these precautionary measures, we believe that our null theta-gamma coupling results might be due to relatively low sensitivity of EEG to gamma-band frequencies⁴⁸. Alternatively, reappraisal and distraction switches could be implemented through dissociable neural circuits^{49–51}. Unfortunately, the insufficient number of switch trials per strategy precludes exploring this possibility in the current study. It is also possible that in our task the switching decision reflected behavioral expression of the intention to switch to an alternative strategy (upon stimulus re-encounter) and that FPI interacted with PPC at some later post-choice (pre-)implementation phase of the trial (see Fig. 1D). Future studies might thus use techniques that are more sensitive to high-frequency activity (e.g. MEG), increase the number of trials per strategy (e.g., by shortening the trial duration), and instruct participants to switch (or maintain) strategies immediately upon the decision (i.e., response delivery) to increase the chances of detecting downstream region(s) with which FPI interacts to implement the switches.

It would be also interesting to examine in future studies how counterfactual computations in FPI might be integrated with computations of other brain circuits involved in cognitive control and decision-making. For instance, a recent study suggested that distinct frontoparietal theta networks are associated with switch-related, proactive control processes, and interference-related, reactive control processes⁵². It would be thus interesting to measure connectivity between FPI and proactive/reactive cognitive control networks. Moreover, given that FPI exerts control over the most integrated aspects of information processing, it would be interesting to measure efferent projections from FPI towards higher-order association areas with which FPI it is densely and reciprocally connected^{53,54}. Finally, FPI theta-band activity has been associated with prospective memory, i.e., forming intentions toward future behaviour¹⁵, mental simulation and execution of planned behavior⁵⁵, and metacognition, that is monitoring and evaluation of one's own cognitive processes^{13,14}. It would thus be interesting to parse these processes in future studies on emotion regulation strategy-switching to see how they relate to FPI theta-band activity and its connectivity with other downstream regions.

Role of the FPM and the reasons for switching strategies

Our study also did not reveal the theta-band increase in FPM activity, which has been proposed to reflect monitoring of the benefit of the current strategy^{3,4,9}. This might be because participants sometimes select strategies that are less effective in achieving the desired emotion regulation goal. Specifically, in this study participants predominantly decided to maintain reappraisal for high affordance stimuli, even though reappraisal was overall less effective than distraction, in terms of downregulation effects^{20,56}. This suggests that factors other than immediate strategy efficacy may contribute to the decision to maintain (and switch) an emotion regulation strategy. For instance, participants may decide to maintain strategies to avoid task-switching effort⁵⁷ or to get a second chance to implement the same strategy in an alternative way (i.e., using a different 'tactic')^{58,59}. Although in this study we did observe adaptive, context-sensitive strategy-switching decisions¹, participants decided to maintain the initial strategy on most of the trials. This is in line with previous studies on flexible emotion regulation decisions²⁷, and a recent research which suggests that people preferably choose recently or frequently employed emotion regulation strategies⁵⁷. An influence of other factors beyond strategy efficacy on emotion regulation decisions could potentially explain the lack of increased FPM activity in the maintain condition. Future studies would benefit from controlling the impact of such other factors, for instance, by asking participants about their motivations for switching (or maintaining) a particular emotion regulation strategy on some trials.

Clinical implications

Aberrant FPI function has been reported in various clinical conditions. For instance, FPI shows hyperactivity at rest, but hypoactivity during implementation of social-emotional action control in socially anxious⁶ or psychopathic individuals⁶⁰. Moreover, FPI shows abnormal connectivity with the reward system in individuals with major depression disorder⁶¹. By contrast, increased activity in left FPI (both at rest and during reappraisal-based emotion regulation) has been reported as the most prominent and clinically relevant brain change following successful treatment for post-traumatic stress disorder (PTSD)⁶². Relatedly, increased frontopolar activity during emotional control before exposure to a traumatic event has been associated with lower PTSD symptoms after traumatic exposure⁶³. Our study suggests that FPI function is involved in context-sensitive modulation of emotional control and may thus serve as a transdiagnostic neural target for stimulation-based therapies for affective disorders involving deficient recruitment of this region. Improving flexible emotional control could be achieved by targeting FPI using transcranial direct current (tDCS) or magnetic stimulation (TMS)^{64–68}, or, once the downstream region with which FPI interacts is identified, by targeting long-range phase-amplitude neuronal coupling between FPI and the brain circuit implementing strategy switches using dual-site transcranial alternating current stimulation (tACS). This latter approach has already shown promising results increasing the efficacy of frontopolar control over automatic action tendencies in favor of alternative, rule-based actions in both healthy⁵ and socially anxious populations⁶⁹.

Conclusion

This study provides a possible mechanism by which cortical oscillatory processes support flexible switching between alternative cognitive emotion regulation strategies. Prior to switch decisions, theta-band power increases over FPI, potentially reflecting evaluation of the efficacy of the alternative relative to the current emotion

regulation strategy. This finding furthers our understanding of the neural mechanism underlying flexible use of emotion regulation strategies and provides a promising neural target for stimulation-based therapies aimed at enhancing emotion regulation flexibility in affective psychopathologies.

Method

Participants

Sixty-three Jagiellonian University students (or recent graduates) took part in this experiment ($M_{\text{age}} = 24.8$, $SD = 4.2$, range 19–37). Based on an a priori sample size calculation, 39 participants were needed to detect an interaction effect (odds ratio = 15.50–16, based on the results of a prior study on strategy-switching by²⁷, and our pilot study) including two categorical predictors on a binary outcome variable decision using logistic regression analysis (see the point M3 in the preregistration for details: <https://osf.io/ze8mg>). We chose to oversample and test at least 60 participants in case of participant dropouts, EEG data collection failure, or excessive EEG artifacts. Because of planned source reconstruction analyses we recruited participants who had an anatomical brain scan from their past participation in an (f)MRI study at MCB Neuroimaging Center, Jagiellonian University. Only female participants were recruited to control for gender differences in emotional picture processing⁷⁰ and the use of emotion regulation⁷¹. All participants had normal or corrected to normal vision and no self-reported history of neurological or psychiatric disorders. One participant was excluded from analyses due to substantial noise in the EEG data (variance of anterior prefrontal channels $> 10^3$) and one due to insufficient trials per condition (preregistered $N_{\text{trials}} < 12$). One participant was excluded due to a problem with triggers during recording. Three additional participants were excluded from time–frequency gamma-band cluster analysis at the channel level due to movement-related artifacts in the gamma range (i.e., an increase in broadband gamma activity around the time of the response). Sixty and 57 participants were thus included in theta-band and gamma-band analyses at the channel level, respectively, and 56 in the analyses at the source level (out of 58 for whom anatomical scans were available). Behavioral and EMG data analyses were performed for all participants included in the theta-band analysis at the channel level, excluding two participants identified as outliers in the EMG analysis (with absolute values larger than $2/\sqrt{N}$ for df betas and $4/N$ for cooks' distances, where N = grouping units⁷², as preregistered: <https://osf.io/ze8mg>) and one participant for whom the EMG signal was not recorded (resulting $N = 57$). In accordance with the Declaration of Helsinki, all procedures were carried out with the adequate understanding and written consent of the participants. Participants received monetary compensation (€15). The study was approved by the ethics committee of Jagiellonian University (KE/21_2022).

Stimuli

Two hundred unpleasant (normative valence: $M = 2.7$, $SD = 0.8$; range: 1 = unpleasant, 7 = pleasant) and arousing (normative arousal: $M = 6.2$, $SD = 0.8$, range: 1 = calm, 7 = aroused) pictures derived from standardized pictorial databases (IAPS⁷³, NAPS⁷⁴, EmoPics⁷⁵) were used. Pictures were divided into high and low reappraisal affordance categories (see Fig. 1A), based on subjective reappraisal difficulty and efficacy ratings (i.e., how easy/difficult and how effective/ineffective reappraisal was), which was determined in a two-part pilot study (part 1: $N = 61$; part 2: $N = 52$ participants; see preregistration for details: <https://osf.io/ze8mg>). These two categories were further divided into two equal sets ($N = 50$ pictures per set), one per strategy. Between categories the sets were equated for normative arousal, and within each category for reappraisal difficulty and efficacy. To avoid low-level visual effects on EEG measures, all pictures were equalized for luminance, contrast, and spatial frequencies. Picture codes as well as individual affordance ratings of high and low affordance pictures are included in our previous report²⁰.

Emotion regulation strategy switching task

In each trial, participants briefly watched a negative picture (passive watch phase) with a high or low reappraisal affordance level. After that participants were instructed to implement a given strategy (reappraisal or distraction) to downregulate their emotional response to the picture (initial implementation phase). Next, they decided to maintain the instructed strategy or to switch to the alternative strategy (decision: switch, maintain), and then implemented this chosen strategy. See Fig. 1D for timing of the trial procedure. Participants received detailed task instructions on how to downregulate their emotional responses (negative affect and emotional arousal) using reappraisal and distraction. We used a situation-focused reappraisal strategy which involves engaging attention to the pictures to change their affective meaning to a more neutral one (see also:^{27,31,32,56}). For reappraisal, participants were instructed to think of the depicted situation as being less negative than it initially seemed, or to think that the situation would end well (despite looking bad or dangerous). Participants were asked not to distance themselves from the situation, e.g., by using reality challenge reappraisals (i.e., interpret emotional events as fake⁵⁸) as this form of reappraisal relies less on the processing content of the stimulus which makes it more similar to distraction²⁵. For distraction, participants were instructed to think of something neutral and unrelated to the picture, such as walking around the neighborhood or performing neutral household chores, while keeping their eyes on the picture. In the passive watch phase, participants were instructed to allow natural thoughts and feelings to arise while looking at the pictures. Instructions were adapted from Sheppes et al. (2014). After these instructions, participants completed several experimenter-guided trials (min. 4, but the exact number depended on each participants' task understanding), during which they implemented each strategy out loud. It was explained to participants that they should switch to an alternative strategy if they: (i) failed to perform the strategy, (ii) felt the current strategy was ineffective, or (iii) preferred to use the other strategy. Then, participants performed nine practice trials to familiarize themselves with the procedure timing. During the practice trials, participants were asked to monitor the efficacy of reappraisal and distraction and to try out switching from one strategy to another. They were also reminded not to close or avert their eyes away from the screen when viewing

the pictures. After that, sensors were attached. Before starting the experimental procedure, we collected a 3D scan of electrode positions. Testing was conducted in a dimly lit, sound-attenuated, air-conditioned EEG cabin.

Several measures were taken to maximize task adherence. First, all participants were informed in advance that the study would involve viewing highly negative and arousing pictures. Second, during training, participants were explicitly instructed not to avert their eyes away from the screen when viewing the pictures, and this was continuously monitored by the research assistants via an online camera. Third, participants were extensively trained in the use of both strategies, and it was verified during the training whether participants found the task feasible within the allotted time (all participants confirmed that it was). Finally, there was a longer break (self-paced) after the completion of the first half of the task. During this break, we verified again whether participants managed to perform the task and rewarded participants with a surprise snack. This gesture aimed to promote task compliance and prolong engagement with the task. Exploratory analyses of the time-on-task effects revealed no difference in the mean number of switch decisions per participant between the first ($M_{\text{switch trials}} = 30.8$) and the second half of the task ($M_{\text{switch trials}} = 30.6$), $p = 0.82$, which confirms the mitigated impact of potential fatigue or practice on regulatory decisions.

The experimental task lasted ~60 min. and consisted of 200 trials, separated by a one-minute break after every 50 trials. The task was administered on a computer equipped with a 61-cm (24 inch) full-HD (i.e., 1920×1080 pixels) resolution LED monitor at a viewing distance of approximately 60 cm and 50° of horizontal visual angle. The pictures were presented full screen. PsychoPy software, version v2021.1.4⁷⁶, was used to control the presentation and timing of stimuli. Further details of the methods are available in our previous report²⁰.

MRI data acquisition

High-resolution, whole-brain anatomical images were acquired using a 3 T scanner (Magnetom Skyra, Siemens). A multi-parameter mapping (MPM) protocol composed of three multi-echo FLASH sequences with MT, T1, and PD contrast weightings was used to acquire MRI data for 40 participants (TR: 18 ms; flip angles for MT, PD, and T1-weighted contrasts: 6° , 4° , 25° , respectively; six equidistant echoes [TE: from 2.46 to 14.76 ms]; 1 mm isotropic reconstruction voxel size; readout FoV: 256 mm; 176 slices). Additional scans for bias correction included mapping of the radiofrequency (RF) transmit (B1+) and receive fields (B1-). For 18 participants MRI data were acquired using a T1-weighted MPRAGE sequence (TR: 1800 ms, flip angle: 8° ; TE: 2.32 ms; 0.9 mm isotropic voxel size; FoV: 256 mm; 208 sagittal slices). A gradient field map was acquired with a dual-echo gradient-echo sequence (TE1 = 4.92 ms, TE2 = 7.3 ms, TR: 503 ms, flip angle = 60°).

Electrophysiological data recording

EEG and EMG signals were recorded using the BioSemi ActiveTwo system (BioSemi, Amsterdam, Netherlands) with ActiView software. Continuous EEG was recorded from 64 electrodes based on the extended 10/20 system, using an ECI Electrocap, as well as two electrodes placed on the left and right mastoids. Vertical and horizontal eye movements were recorded with electrodes placed supra- and infra-orbitally at the right eye and on the left versus right orbital rim. The Common Mode Sense (CMS) active electrode and the Driven Right Leg (DRL) passive electrode formed the amplifier reference during recording. The EMG signal was recorded from the corrugator supercilii (frown muscles) using Ag/AgCl electrodes with saline based electrode gel and a bipolar placement according to the guidelines provided by Fridlund and Cacioppo⁷⁷. All signals were sampled at 1024 Hz. 3D scans of EEG electrode positions were acquired using the Structure Channel from Occipital (Boulder, CO) to improve the spatial accuracy of individual source models⁷⁸.

EMG: pre-processing, data reduction and analysis

The bipolar EMG signal was calculated in the initial implementation phase (see Fig. 1D) by taking the difference between the two EMG electrodes. This signal was then filtered in a range of 20–400 Hz with a Butterworth two-pass zero-phase IIR filter (order: 9, window type: Hamming), and a discrete Fourier transform filter (to remove the 50 Hz line noise and 100 and 150 Hz harmonics), rectified (by taking the absolute values), smoothed with a 20-Hz low-pass filter, and downsampled to 512 Hz. These steps were implemented in FieldTrip⁷⁹. We quantified the amplitude of the corrugator as percentage of signal change in the initial implementation phase between 0.45 s after picture onset until 3 s (the end of picture presentation) compared to the mean baseline activity, defined as an average corrugator activity between -0.2 s to 0 s relative to picture onset, ($[\text{post-stimulus} - \text{baseline}] * 100 / \text{baseline}$)⁸⁰.

EEG pre-processing

EEG analyses were performed using MATLAB2021a (The MathWorks), Fieldtrip toolbox⁷⁹, and custom-written analysis scripts. As preregistered, we analyzed picture-locked EEG activity in the initial implementation phase and response-locked EEG activity in the decision phase (see Fig. 1D). Data were segmented into epochs starting from -0.5 s to 3.5 s relative to picture onset in the initial implementation phase and -1.5 s to 0.5 s relative to response onset in the decision phase ($M_{\text{reaction time}} = 1.60$ s, $SD = 2.57$ s). The epochs were demeaned to remove nonzero DC offset, filtered using a discrete Fourier transform filter to remove the 50 Hz line noise and 100 and 150 Hz harmonics and a low-pass Butterworth IIR filter (order: 9, type: Hamming) with a cut-off of 100 Hz, re-referenced to the average activity of two mastoids, and downsampled to 256 Hz. Next, manual trial rejection was performed to remove trials with large deviations or artifacts. Independent component analysis was then performed to remove components that contained sources of noise (e.g., eye blinks, saccades, muscle artifacts) [81]. After this step, all trials were inspected visually to remove any trials still containing visible artifacts. The average number of retained trials was 195.1 (97.5%; $M_{\text{maintain trials}} = 133.7$ and $M_{\text{switch trials}} = 61.4$).

Time–frequency analyses

Time–frequency representations (TFR) of power were estimated in two steps. For frequencies below 40 Hz, we used short-time Fourier transform with sliding windows of 500 ms, multiplied with a Hanning taper and moving in steps of 50 ms. The frequency resolution was 1 Hz. For frequencies above 40 Hz, we used three orthogonal Slepian tapers and sliding time windows of 200 ms (moving in steps of 50 ms), creating frequency smoothing of 10 Hz¹⁰. The frequency resolution was 5 Hz. In the initial implementation phase, we tested differences in activity between 0 to 3 s relative to picture onset compared to a baseline period defined as an average activity between -0.2 s to 0 s relative to picture onset. In the decision phase, we tested for theta-band activity evoked 1 s before to 0.2 s after the response relative to a baseline period defined as an average activity between 1.2 s to 1 s before the response. Because there was no difference in theta-band power versus baseline in frontal channels in the implementation phase, we restricted our further analyses to the decision phase (see Results).

Source reconstruction analyses

Sources of the switch effects (i.e., condition differences in theta and gamma power) were localized using dynamic imaging of coherent sources (DICS) beamforming⁸². We computed a finite element method (FEM), 5-shell head model for each subject using anatomical MRI. Next, we warped the individual MRI images to a template grid in MNI space (spatial resolution of 10 mm). Individual source models were computed using the recorded 3D scans of EEG electrode positions. Prior to the spectral decomposition, the signal was re-referenced to the common average reference. Activity was reconstructed using multi-taper FFT in time intervals and frequency ranges for which significant effects were observed at the channel level (i.e., 4 Hz \pm 2 Hz of smoothing for theta; see Results). A common spatial filter was created for each frequency based on all trials. This filter was consequently applied to switch and maintain trials separately. We computed the relative change in power for switch versus maintain trials (switch-maintain)/(switch + maintain) to assess differences between conditions. Region labeling was done based on the Harvard–Oxford cortical structural atlas implemented in FSL (https://fsl.fmrib.ox.ac.uk/fsl/fslwiki/i/;RRID:SCR_002823).

Spatial filters applied to ROIs

We used a linearly constrained minimum variance (LCMV) beamforming⁸³ to create spatial filters for extracting the signal time courses from FPI and PPC. For a phase-providing signal, the time-series was reconstructed from a local maximum grid point corresponding to FPI [left frontal pole (MNI: -32 66 0)] resulting from the group-level source reconstruction analysis of the theta-band switch effects. PPC time-series were reconstructed from the left PPC defined as the average activity of the left superior and inferior parietal lobules based on automated anatomical labeling (AAL) atlas⁸⁴. To explore phase synchronization between FPI and SMG, which showed the theta power increase in the switch vs. maintain condition, we reconstructed signal time-series from a local maximum grid point corresponding to left superior temporal gyrus/supramarginal gyrus [SMG (MNI: -52 -44 16)] resulting from the group-level source reconstruction analysis of the theta-band switch effects.

Connectivity analysis. To assess whether FPI synchronizes activity with the PPC before the decision to switch from vs. maintain the instructed emotion regulation strategy, we calculated an index of phase-amplitude coupling based on the Modulation Index⁴⁰, in the time window in which a significant theta-power increase was observed across conditions compared to baseline (i.e., 0.95 s before to 0.20 s after the response). This longer time-window was used to allow the reconstruction of 4 Hz theta oscillations (i.e., the center frequency between 2–6 Hz). To control for potential biases in phase-based analyses due to lower trial counts for the switch as compared to the maintain condition, we randomly sampled trials from the maintain condition to equate the number of trials used in both analyses. This procedure was repeated 100 times for increased reliability of estimates (see Statistical analyses section for details). The signals extracted from FPI (MNI: -32 66 0) and SMG (-52 -44 16) were decomposed into a theta-band 4 Hz complex signals using STFFT with a 500 ms window tapered with a Hanning filter and moving in steps of 1 ms (frequency resolution = 1 Hz). The signal extracted from the PPC was decomposed into a gamma-band (40–90 Hz) complex signal using STFFT with a 200 ms window tapered with a Hanning window containing six cycles per frequency band ($dT=6/f$) and moving in steps of 1 ms (frequency resolution = 5 Hz). As a follow-up analysis we computed an estimate of neural excitability by calculating the slope of the power spectrum between 30–50 Hz from the signal extracted from PPC, locked to FPI theta-band peak and trough time windows⁴¹. We compared these estimates between switch and maintain trials. Phase synchrony between FPI and SMG was estimated using the imaginary part of coherency to suppress spurious coherency driven by electromagnetic field spread^{42,85} as well as phase-slope index (PSI), an index that allows to detect direction of information flow between brain regions.

Statistical analyses

The behavioral and EMG data were analyzed with a frequentist (generalized) linear mixed-effects model approach (G/LMM), using lmer (for continuous dependent variables (DV) and glmer (for binary DV) functions of the lme4 package, version 1.1.31⁸⁶, and the function mixed of the afex package, version 1.2.0 (for Type III Likelihood Ratio Tests for the binary DV⁸⁷) implemented in R, version 4.2.2⁸⁸. Because the psychophysiological data were aggregated over trials to increase the signal-to-noise ratio, the averaged corrugator amplitudes per condition were included as *dependent variables* in the analyses, and the conditions (Instructed Strategy x Decision) as *predictors*. Hence, if corrugator amplitudes in the initial strategy implementation phases predict switch decisions, this is reflected in the amplitude differences between switch vs. maintain trials. We followed the approach of fitting maximal models⁸⁹, i.e., including all random intercepts, slopes, and correlations justified by the experimental design. The critical alpha level for determining statistical significance for a frequentist (G) LMM effect was $p < 0.05$ (corrected for multiple comparisons for post-hoc tests using FDR correction). Cohen's

d and parameter estimates are reported to present the magnitude of effects. We report results for full-random effect (G)LMMs, excluding outliers identified with df betas and cooks' distances (as preregistered).

Statistical analyses on the channel and source level consisted of cluster-based nonparametric permutation tests^{90,91}. This procedure ensures correction for multiple comparisons over time, channels, and frequencies accounting for the spatio-spectral-temporal dependency in the data. As test statistics, we used t -values. The significance probability was calculated using the Monte Carlo method (10,000 permutations). The relationship between FPI theta-band phase and PPC gamma-band power was assessed by calculating the Kullback-Liebler (KL)-based Modulation Index (MI)⁴⁰. This index computes the deviation from a uniform distribution of higher frequency amplitude values as a function of a lower frequency phase signal using KL divergence and is the most robust for short data segments and low signal-to-noise ratio among alternative methods of measuring phase-amplitude coupling (PAC)⁹². The relationship between FPI and SMG theta-band signals was assessed by calculating the imaginary part of coherency (iCoh)⁴² and phase-slope index (PSI)⁴³. The iCoh value ranges from 0 to 1 and reflects the consistency of the phase difference between two signals at a given frequency. The PSI estimates the direction of information flow between two signals. A positive PSI indicates that the region acts as a sender, and a negative value that it acts as a receiver. To ensure that condition differences in PAC, iCoh, and PSI were not dependent on the specific (random) selection of maintain trials, condition differences in all connectivity metrics were estimated 100 times, each time using a different random subset of maintain trials. The averages of these condition differences were then used for statistical testing.

Data availability

The datasets that support the findings of the current study and the code used to generate them will be made available in the Radboud Data Repository (<https://data.ru.nl/>) upon completion of the project.

Received: 11 September 2024; Accepted: 18 February 2025

Published online: 29 March 2025

References

- Bonanno, G. A. & Burton, C. L. Regulatory flexibility: An individual differences perspective on coping and emotion regulation. *Perspect. Psychol. Sci.* **8**, 591–612 (2013).
- Sheppes, G., Suri, G. & Gross, J. J. Emotion regulation and psychopathology. *Annu. Rev. Clin. Psychol.* **11**, 379–405 (2015).
- Mansouri, F. A., Koechlin, E., Rosa, M. G. P. & Buckley, M. J. Managing competing goals - A key role for the frontopolar cortex. *Nat. Rev. Neurosci.* **18**, 645–657 (2017).
- Koch, S. B. J., Mars, R. B., Toni, I. & Roelofs, K. Emotional control, reappraised. *Neurosci. Biobehav. Rev.* **95**, 528–534 (2018).
- Bramson, B., den Ouden, H. E., Toni, I. & Roelofs, K. Improving emotional-action control by targeting long-range phase-amplitude neuronal coupling. *eLife* **9**, e59600 (2020).
- Bramson, B., Meijer, S., van Nuland, A., Toni, I. & Roelofs, K. Anxious individuals shift emotion control from lateral frontal pole to dorsolateral prefrontal cortex. *Nat. Commun.* **14**, 4880 (2023).
- Boorman, E. D., Behrens, T. E. J., Woolrich, M. W. & Rushworth, M. F. S. How green is the grass on the other side? Frontopolar cortex and the evidence in favor of alternative courses of action. *Neuron* **62**, 733–743 (2009).
- Boorman, E. D., Behrens, T. E. & Rushworth, M. F. Counterfactual choice and learning in a neural network centered on human lateral frontopolar cortex. *PLoS Biol.* **9**, e1001093 (2011).
- Roelofs, K., Bramson, B. & Toni, I. A neurocognitive theory of flexible emotion control: The role of the lateral frontal pole in emotion regulation. *Ann. N. Y. Acad. Sci.* **1525**, 28–40 (2023).
- Bramson, B., Jensen, O., Toni, I. & Roelofs, K. Cortical oscillatory mechanisms supporting the control of human social-emotional actions. *J. Neurosci.* **38**, 5739–5749 (2018).
- Cavanagh, J. F., Figueroa, C. M., Cohen, M. X. & Frank, M. J. Frontal theta reflects uncertainty and unexpectedness during exploration and exploitation. *Cereb. Cortex* **22**, 2575–2586 (2012).
- Voytek, B. et al. Oscillatory dynamics coordinating human frontal networks in support of goal maintenance. *Nat. Neurosci.* **18**, 1318–1324 (2015).
- Wokke, M. E., Cleeremans, A. & Ridderinkhof, K. R. Sure I'm sure: Prefrontal oscillations support metacognitive monitoring of decision making. *J. Neurosci.* **37**, 781–789 (2017).
- Soutschek, A., Moisa, M., Ruff, C. C. & Tobler, P. N. Frontopolar theta oscillations link metacognition with prospective decision making. *Nat. Commun.* **12**, 3943 (2021).
- Domic-Siede, M., Irani, M., Valdés, J., Perrone-Bertolotti, M. & Ossandón, T. Theta activity from frontopolar cortex, mid-cingulate cortex and anterior cingulate cortex shows different roles in cognitive planning performance. *NeuroImage* **226**, 117557 (2021).
- Costa, A. et al. the right frontopolar cortex is involved in visual-spatial prospective memory. *PLOS ONE* **8**, e56039 (2013).
- Lisman, J. E. & Jensen, O. The θ - γ neural code. *Neuron* **77**, 1002–1016 (2013).
- Lapate, R. C., Ballard, I. C., Heckner, M. K. & D'Esposito, M. Emotional context sculpts action goal representations in the lateral frontal pole. *J. Neurosci.* **42**, 1529–1541 (2022).
- Badre, D., Bhandari, A., Keglovits, H. & Kikumoto, A. The dimensionality of neural representations for control. *Curr. Opin. Behav. Sci.* **38**, 20–28 (2021).
- Adamczyk, A. K., Koch, S. B. J., Wyczesany, M., Roelofs, K. & van Peer, J. M. Emotion regulation flexibility: EEG/EMG predictors and consequences of switching between reappraisal and distraction strategies. *Psychophysiology* e14646 (2024). <https://doi.org/10.1111/psyp.14646>.
- Etkin, A., Büchel, C. & Gross, J. J. The neural bases of emotion regulation. *Nat. Rev. Neurosci.* **16**, 693–700 (2015).
- McRae, K. Cognitive emotion regulation: A review of theory and scientific findings. *Curr. Opin. Behav. Sci.* **10**, 119–124 (2016).
- Ochsner, K. & Gross, J. The cognitive control of emotion. *Trends Cognit. Sci.* **9**, 242–249 (2005).
- Ochsner, K. N. et al. For better or for worse: Neural systems supporting the cognitive down- and up-regulation of negative emotion. *NeuroImage* **23**, 483–499 (2004).
- Sheppes, G. et al. Emotion regulation choice: A conceptual framework and supporting evidence. *J. Exp. Psychol. Gen.* **143**, 163–181 (2014).
- Birk, J. L. & Bonanno, G. A. When to throw the switch: The adaptiveness of modifying emotion regulation strategies based on affective and physiological feedback. *Emotion* **16**, 657–670 (2016).
- Dorman Ilan, S., Shafir, R., Birk, J. L., Bonanno, G. A. & Sheppes, G. Monitoring in emotion regulation: behavioral decisions and neural consequences. *Soc. Cognit. Affect. Neurosci.* **14**, 1273–1283 (2019).

28. Dryman, M. T. & Heimberg, R. G. Emotion regulation in social anxiety and depression: A systematic review of expressive suppression and cognitive reappraisal. *Clin. Psychol. Rev.* **65**, 17–42 (2018).
29. de Voogd, L. D., Hermans, E. J. & Phelps, E. A. Regulating defensive survival circuits through cognitive demand via large-scale network reorganization. *Curr. Opin. Behav. Sci.* **24**, 124–129 (2018).
30. Adamczyk, A. K., Wyczesany, M. & van Peer, J. M. High working memory load impairs reappraisal but facilitates distraction – An event-related potential investigation. *Biol. Psychol.* 108327 (2022) <https://doi.org/10.1016/j.biopsycho.2022.108327>.
31. Shafir, R., Schwartz, N., Blechert, J. & Sheppes, G. Emotional intensity influences pre-implementation and implementation of distraction and reappraisal. *Soc. Cognit. Affect. Neurosci.* **10**, 1329–1337 (2015).
32. Shafir, R., Thiruchselvam, R., Suri, G., Gross, J. J. & Sheppes, G. Neural processing of emotional-intensity predicts emotion regulation choice. *Soc. Cognit. Affect. Neurosci.* **11**, 1863–1871 (2016).
33. Suri, G. et al. Emotion regulation choice: The role of environmental affordances. *Cognit. Emot.* **32**, 963–971 (2018).
34. Young, G. & Suri, G. Emotion regulation choice: A broad examination of external factors. *Cognit. Emot.* **34**, 242–261 (2020).
35. Dimberg, U. Facial reactions to facial expressions. *Psychophysiology* **19**, 643–647 (1982).
36. Ray, R. D., McRae, K., Ochsner, K. N. & Gross, J. J. Cognitive reappraisal of negative affect: Converging evidence from EMG and self-report. *Emotion* **10**, 587–592 (2010).
37. Urry, H. L. Seeing, thinking, and feeling: Emotion-regulating effects of gaze-directed cognitive reappraisal. *Emotion* **10**, 125–135 (2010).
38. Kreibitz, S. D., Brown, A. S. & Gross, J. J. Quantitative versus qualitative emotion regulation goals: Differential effects on emotional responses. *Psychophysiology* **60**, e14387 (2023).
39. Buzsáki, G. & Wang, X.-J. Mechanisms of gamma oscillations. *Annu. Rev. Neurosci.* **35**, 203–225 (2012).
40. Tort, A. B. L., Komorowski, R., Eichenbaum, H. & Kopell, N. Measuring phase-amplitude coupling between neuronal oscillations of different frequencies. *J. Neurophysiol.* **104**, 1195–1210 (2010).
41. Gao, R., Peterson, E. J. & Voytek, B. Inferring synaptic excitation/inhibition balance from field potentials. *NeuroImage* **158**, 70–78 (2017).
42. Nolte, G. et al. Identifying true brain interaction from EEG data using the imaginary part of coherency. *Clin. Neurophysiol.* **115**, 2292–2307 (2004).
43. Nolte, G. et al. Robustly estimating the flow direction of information in complex physical systems. *Phys. Rev. Lett.* **100**, 234101 (2008).
44. Neubert, F.-X., Mars, R. B., Thomas, A. G., Sallet, J. & Rushworth, M. F. S. Comparison of human ventral frontal cortex areas for cognitive control and language with areas in monkey frontal cortex. *Neuron* **81**, 700–713 (2014).
45. Folloni, D. et al. Dichotomous organization of amygdala/temporal-prefrontal bundles in both humans and monkeys. *eLife* **8**, e47175 (2019).
46. Volman, I., Roelofs, K., Koch, S., Verhagen, L. & Toni, I. Anterior prefrontal cortex inhibition impairs control over social emotional actions. *Curr. Biol.* **21**, 1766–1770 (2011).
47. Weber, J. et al. Ramping dynamics and theta oscillations reflect dissociable signatures during rule-guided human behavior. *Nat. Commun.* **15**, 637 (2024).
48. Oostendorp, T. F., Delbeke, J. & Stegeman, D. F. The conductivity of the human skull: Results of in vivo and in vitro measurements. *IEEE Trans. Biomed. Eng.* **47**, 1487–1492 (2000).
49. Morawetz, C., Bode, S., Derntl, B. & Heekeren, H. R. The effect of strategies, goals and stimulus material on the neural mechanisms of emotion regulation: A meta-analysis of fMRI studies. *Neurosci. Biobehav. Rev.* **72**, 111–128 (2017).
50. Kanske, P., Heissler, J., Schönfelder, S., Bongers, A. & Wessa, M. How to regulate emotion? Neural networks for reappraisal and distraction. *Cerebral Cortex* **21**, 1379–1388 (2011).
51. McRae, K. et al. The neural bases of distraction and reappraisal. *J. Cognit. Neurosci.* **22**, 248–262 (2010).
52. Cooper, P. S. et al. Theta frontoparietal connectivity associated with proactive and reactive cognitive control processes. *NeuroImage* **108**, 354–363 (2015).
53. Petrides, M. & Pandya, D. N. Efferent association pathways from the rostral prefrontal cortex in the Macaque monkey. *J. Neurosci.* **27**, 11573–11586 (2007).
54. Koch, S. B. J. et al. Neural control of emotional actions in response to affective vocalizations. *J. Cogn. Neurosci.* **32**, 977–988 (2020).
55. Addis, D. R., Wong, A. T. & Schacter, D. L. Remembering the past and imagining the future: Common and distinct neural substrates during event construction and elaboration. *Neuropsychologia* **45**, 1363–1377 (2007).
56. Adamczyk, A. K., Wyczesany, M., Roelofs, K. & van Peer, J. M. Reappraisal is less effective than distraction in downregulation of neural responses to physical threats—An event-related potential investigation. *Psychophysiology* e14316 (2023). <https://doi.org/10.1111/psyp.14316>.
57. Ghafur, R. D., Suri, G. & Gross, J. J. Emotion regulation choice: The role of orienting attention and action readiness. *Curr. Opin. Behav. Sci.* **19**, 31–35 (2018).
58. McRae, K., Ciesielski, B. & Gross, J. J. Unpacking cognitive reappraisal: Goals, tactics, and outcomes. *Emotion* **12**, 250–255 (2012).
59. Webb, T. L., Miles, E. & Sheeran, P. Dealing with feeling: A meta-analysis of the effectiveness of strategies derived from the process model of emotion regulation. *Psychol. Bull.* **138**, 775–808 (2012).
60. Volman, I. et al. Testosterone modulates altered prefrontal control of emotional actions in psychopathic offenders. *eNeuro* **3**, ENEURO.0107-15.2016 (2016).
61. Fettes, P. W. et al. Abnormal functional connectivity of frontopolar subregions in treatment-nonresponsive major depressive disorder. *Biol. Psychiatry Cognit. Neurosci. Neuroimaging* **3**, 337–347 (2018).
62. Fonzo, G. A. et al. Selective effects of psychotherapy on frontopolar cortical function in PTSD. *Am. J. Psychiatry* **174**, 1175–1184 (2017).
63. Kaldewaij, R. et al. Anterior prefrontal brain activity during emotion control predicts resilience to post-traumatic stress symptoms. *Nat. Hum. Behav.* **5**, 1055–1064 (2021).
64. Mutz, J., Edgcombe, D. R., Brunoni, A. R. & Fu, C. H. Y. Efficacy and acceptability of non-invasive brain stimulation for the treatment of adult unipolar and bipolar depression: A systematic review and meta-analysis of randomised sham-controlled trials. *Neurosci. Biobehav. Rev.* **92**, 291–303 (2018).
65. Smits, F. M., Schutter, D. J. L. G., van Honk, J. & Geuze, E. Does non-invasive brain stimulation modulate emotional stress reactivity? *Soc. Cognit. Affect. Neurosci.* **15**, 23–51 (2020).
66. Vicario, C. M., Salehinejad, M. A., Felmingham, K., Martino, G. & Nitsche, M. A. A systematic review on the therapeutic effectiveness of non-invasive brain stimulation for the treatment of anxiety disorders. *Neurosci. Biobehav. Rev.* **96**, 219–231 (2019).
67. Wyczesany, M. et al. Offline rTMS inhibition of the right dorsolateral prefrontal cortex impairs reappraisal efficacy. *Sci. Rep.* **12**, 21394 (2022).
68. Wyczesany, M. et al. Inhibition of the dorsolateral cortex reveals specific mechanisms behind emotional control. *Biol. Psychol.* **186**, 108743 (2024).
69. Meijer, S., Bramson, B., Toni, I. & Roelofs, K. Improving emotion control in social anxiety by targeting rhythmic brain activity. 2023.09.01.555689. Preprint at <https://doi.org/10.1101/2023.09.01.555689> (2024).
70. Filkowski, M. M., Olsen, R. M., Duda, B., Wanger, T. J. & Sabatinelli, D. Sex differences in emotional perception: Meta analysis of divergent activation. *NeuroImage* **147**, 925–933 (2017).

71. McRae, K., Ochsner, K. N., Mauss, I. B., Gabrieli, J. J. D. & Gross, J. J. Gender differences in emotion regulation: An fMRI study of cognitive reappraisal. *Group Process. Intergroup Relat.* **11**, 143–162 (2008).
72. Nieuwenhuis, R., Grotenhuis, M. te & Pelzer, B. influence.ME: Tools for detecting influential data in mixed effects models. *R. J.* **4**, 38–47 (2012).
73. Lang, P. J., Bradley, M. M. & Cuthbert, B. N. *International Affective Picture System (IAPS): Affective Ratings of Pictures and Instruction Manual. Technical Report A-8.* (University of Florida, 2008).
74. Marchewka, A., Żurawski, Ł., Jednoróg, K. & Grabowska, A. The Nencki Affective Picture System (NAPS): Introduction to a novel, standardized, wide-range, high-quality, realistic picture database. *Behav. Res. Methods* **46**, 596–610 (2014).
75. Wessa, M. et al. EmoPics: Subjektive und psychophysiologische Evaluation neuen Bildmaterials für die klinisch-biopsychologische Forschung. *Z. Klin. Psychol. Psychother.* **39** (2010).
76. Peirce, J. et al. PsychoPy2: Experiments in behavior made easy. *Behav. Res.* **51**, 195–203 (2019).
77. Fridlund, A. J. & Cacioppo, J. T. Guidelines for human electromyographic research. *Psychophysiology* **23**, 567–589 (1986).
78. Homöle, S. & Oostenveld, R. Using a structured-light 3D scanner to improve EEG source modeling with more accurate electrode positions. *J. Neurosci. Methods* **326**, 108378 (2019).
79. Oostenveld, R., Fries, P., Maris, E. & Schoffelen, J.-M. FieldTrip: Open source software for advanced analysis of MEG, EEG, and invasive electrophysiological data. *Comput. Intell. Neurosci.* **2011**, 156869 (2011).
80. van Boxtel, A. Facial EMG as a tool for inferring affective states. In *Proceedings of Measuring Behavior*. 104–108 (2010).
81. Makeig, S., Bell, A., Jung, T.-P. & Sejnowski, T. Independent component analysis of electroencephalographic data. *Adv. Neural Inf. Process. Syst.* **8**, 145–151 (1996).
82. Gross, J. et al. Dynamic imaging of coherent sources: Studying neural interactions in the human brain. *Proc. Natl. Acad. Sci. USA* **98**, 694–699 (2001).
83. van Veen, B. D., van Drongelen, W., Yuchtman, M. & Suzuki, A. Localization of brain electrical activity via linearly constrained minimum variance spatial filtering. *IEEE Trans. Biomed. Eng.* **44**, 867–880 (1997).
84. Tzourio-Mazoyer, N. et al. Automated anatomical labeling of activations in SPM using a macroscopic anatomical parcellation of the MNI MRI single-subject brain. *Neuroimage* **15**, 273–289 (2002).
85. Bastos, A. M. & Schoffelen, J.-M. A Tutorial review of functional connectivity analysis methods and their interpretational pitfalls. *Front. Syst. Neurosci.* **9** (2016).
86. Bates, D., Mächler, M., Bolker, B. & Walker, S. Fitting linear mixed-effects models using lme4. *J. Stat. Softw.* **67**, 1–48 (2015).
87. Singmann, H. et al. *afex: Analysis of Factorial Experiments*. (2022).
88. R Core Team. *R: A Language and Environment for Statistical Computing*. (2021) <http://www.R-project.org/>.
89. Barr, D. J., Levy, R., Scheepers, C. & Tily, H. J. Random effects structure for confirmatory hypothesis testing: Keep it maximal. *J. Mem. Lang.* **68**, 255–278 (2013).
90. Hayasaka, S. & Nichols, T. E. Combining voxel intensity and cluster extent with permutation test framework. *NeuroImage* **23**, 54–63 (2004).
91. Maris, E. & Oostenveld, R. Nonparametric statistical testing of EEG- and MEG-data. *J. Neurosci. Methods* **164**, 177–190 (2007).
92. Hülsemann, M. J., Naumann, E. & Rasch, B. Quantification of phase-amplitude coupling in neuronal oscillations: Comparison of phase-locking value, mean vector length, modulation index, and generalized-linear-modeling-cross-frequency-coupling. *Front. Neurosci.* **13** (2019).

Acknowledgements

We thank (in research-chronological order): research participants for contributing their time and (functional and structural) brains; research assistants: Zofia Domagalska, Zofia Helis, Iwona Przybył, and Oliwia Anusiewicz for help with data collection; principal investigators Zofia Wodniecka-Chlipalska, Michał Wierzechoń, Michał Kuniecki and the research teams of their NCN-funded projects 2017/27/B/HS6/00959, 2017/27/B/HS6/00937, 2012/07/E/HS6/01046, esp. Justyna Hobot, Agata Wolna, Katarzyna Hat, as well as Aleksandra Domagalik, head of the Neuroimaging Center at MCB UJ, for collecting and sharing anatomical brain scans of research the participants; Robert Oostenveld and Jan-Mathijs Schoffelen for analysis tips and suggestions.

Author contributions

Conceptualization: AKA, BB, SBJK, JMP, KR; data curation: AKA, formal analysis: AKA; funding acquisition: AKA; investigation: AKA; methodology: AKA, BB, SBJK, JMP, KR; project administration: AKA; resources: AKA; software: AKA; visualization: AKA; writing—original draft: AKA; writing—review and editing: AKA, BB, SBJK, JMP, KR, MW.

Funding

This research was supported by a grant from the National Science Centre (NCN) in Poland (2018/31/N/HS6/03962), NENS Exchange grant from the Federation of European Neuroscience Societies, an internal grant from the Jagiellonian University (N12/MNW/000038), and the Foundation for Polish Science START Scholarship awarded to Agnieszka K. Adamczyk. Karin Roelofs and Bob Bramson were supported by Consolidator grant DARE2APPROACH from the European Research Council (ERC_CoG_772337) and by a consortium grant from the Dutch Research Council INTENSE (NWO_Crossover_17619).

Declarations

Competing interests

The authors declare no competing interests.

Preregistration

This study's design, hypotheses, and analysis plan were preregistered in accordance with the APA Preregistration for Quantitative Research in Psychology (PRP-QUANT) Template and can be accessed at <https://osf.io/ze8mg>.

Additional information

Correspondence and requests for materials should be addressed to A.K.A.

Reprints and permissions information is available at www.nature.com/reprints.

Publisher's note Springer Nature remains neutral with regard to jurisdictional claims in published maps and institutional affiliations.

Open Access This article is licensed under a Creative Commons Attribution-NonCommercial-NoDerivatives 4.0 International License, which permits any non-commercial use, sharing, distribution and reproduction in any medium or format, as long as you give appropriate credit to the original author(s) and the source, provide a link to the Creative Commons licence, and indicate if you modified the licensed material. You do not have permission under this licence to share adapted material derived from this article or parts of it. The images or other third party material in this article are included in the article's Creative Commons licence, unless indicated otherwise in a credit line to the material. If material is not included in the article's Creative Commons licence and your intended use is not permitted by statutory regulation or exceeds the permitted use, you will need to obtain permission directly from the copyright holder. To view a copy of this licence, visit <http://creativecommons.org/licenses/by-nc-nd/4.0/>.

© The Author(s) 2025